

On a Mixture of the Lindley and Modified Lindley Distributions: Properties and Estimation

Christophe Chesneau^{1*}, Lishamol Tomy² and Jiju Gillarirose³

¹ Université de Caen, LMNO, Campus II, Science 3, 14032, Caen, France

² Department of Statistics, Deva Matha College, Kuravilangad, Kerala, 686633, India

³ Department of Statistics and Data Science, Christ University, Bangalore, Karnataka-560029, India,

Received: May 1, 2024

Accepted : March 11, 2025

Abstract: In this article, we investigate a novel three-parameter lifetime distribution constructed from a mixture of the original Lindley and modified Lindley distributions. The concept behind this construction is to combine the contrasting properties of these two well-known distributions to provide a new statistical modeling option for lifetime data analysis. In particular, it provides a natural alternative to the three-parameter, two-component mixture of the Lindley distribution, which has attracted attention in the recent statistical literature. We investigate its main properties from both a theoretical and practical point of view. The shapes of the corresponding probability density and hazard rate functions and the formulas for the moments, moment generating functions and characteristic functions are discussed. The distribution is then subjected to statistical analysis, considering it as a semi-parametric model. The maximum likelihood approach is used to estimate the parameters. In a simulation analysis, the numerical behavior of the bias and the mean square error of the obtained estimates are studied. The new model is tested on three data sets and the results show that it has a better fit behavior than its main competitor, the three-parameter two-component mixture of the Lindley model.

Keywords: Lindley distributions; maximum likelihood estimates; mixture distribution; modified Lindley distribution; moments.

2010 Mathematics Subject Classification. 26A25; 26A35.

1 Introduction

The Lindley (L) distribution, introduced by [13], has been widely used in recent decades in fields as diverse as biology, insurance, lifetime analysis and reliability. The corresponding cumulative distribution function (CDF) is defined as follows:

$$F_L(x; \theta) = 1 - \left[1 + \frac{\theta x}{1 + \theta} \right] e^{-\theta x}, \quad x > 0, \quad (1)$$

where $\theta > 0$, and $F_L(x; \theta) = 0$ for $x \leq 0$. The L distribution thus depends on a single scale parameter, and its CDF can be represented as a linear combination of the CDFs of the exponential and gamma distributions. A key characteristic is that its hazard rate function (HRF) is increasing, unlike that of the exponential distribution, which is constant. It is therefore a natural alternative for fitting data with such a hazard rate feature. Further details of the Lindley distribution and model can be found in the literature, for example in [27], [15], [21], [8], [19], [20], [22], [28], [10], [17], [3], [1], [5] and [14]. For a comprehensive overview of the Lindley distribution, see [24, 25].

On the other hand, on the same mathematical basis, [6], proposed the modified L (ML) distribution. It is defined with a CDF that can be presented as a plug-in weighted version of the CDF of the L distribution. More precisely, it is indicated as follows:

$$F_{ML}(x; \theta) = 1 - \left[1 + \frac{\theta x}{1 + \theta} e^{-\theta x} \right] e^{-\theta x}, \quad x > 0,$$

* Corresponding author e-mail: christophe.chesneau@gmail.com

where $\theta > 0$, and $F_{ML}(x; \theta) = 0$ for $x \leq 0$. Like the L distribution, the ML distribution depends on a single scale parameter, and its CDF can be represented as a linear combination of the CDFs of the exponential and gamma distributions. The main difference with the L distribution is that the ML distribution has a unimodal HRF, which makes it useful for analyzing data with analogous empirical characteristics. Furthermore, the following first-order stochastic ordering holds: $F_L(x; \theta) \leq F_{ML}(x; \theta)$, $x \in \mathbb{R}$. Given this result, the ML model has been used to fit several relevant practical data sets better than the L model. See [6].

The inspiration for this article comes from an accurate mixture strategy based on the L distribution that was recently investigated in [3]. In this reference, the capabilities of mixing two L distributions with different parameters are examined. The mixture L-L (L-L) distribution is created and defined by the following CDF:

$$F_{L-L}(x; \theta_1, \theta_2, p) = pF_L(x; \theta_1) + (1 - p)F_L(x; \theta_2), \quad (2)$$

where $p \in [0, 1]$, $\theta_1 > 0$ and $\theta_2 > 0$. Obviously, we have $F_{L-L}(x; \theta_1, \theta_2, 0) = F_L(x; \theta_2)$ and $F_{L-L}(x; \theta_1, \theta_2, 1) = F_L(x; \theta_1)$. It is concluded in [3] that the L-L model is a perfect model for fitting data compared to other mixture models, such as a two-component exponential mixture model (see, [11]), a two-component gamma mixture model (see, [26]), or a two-component Weibull mixture model (see, [9]). With this in mind, we try to use this mixture strategy to positively exploit a "functional gap" between the L and ML distributions. The aim is to achieve new modeling purposes and competitive results compared to the capabilities of the L-L distribution in some statistical scenarios. Thus, based on the construction in Equation (2), we propose to investigate the mixture L-ML (L-ML) distribution defined by the following CDF:

$$F_{L-ML}(x; \theta_1, \theta_2, p) = pF_L(x; \theta_1) + (1 - p)F_{ML}(x; \theta_2), \quad x \in \mathbb{R}, \quad (3)$$

where $p \in [0, 1]$, $\theta_1 > 0$ and $\theta_2 > 0$. Obviously, we have $F_{L-ML}(x; \theta_1, \theta_2, 0) = F_{ML}(x; \theta_2)$ and $F_{L-ML}(x; \theta_1, \theta_2, 1) = F_L(x; \theta_1)$, the parameters θ_1 and θ_2 can be different, and the parameter p serves as a connection between the L and ML distributions. This CDF is thus defined as the mixture of the L and ML distributions and the weight p . In an expanded form, for $x > 0$, it can be expressed as

$$\begin{aligned} F_{L-ML}(x; \theta_1, \theta_2, p) &= p \left\{ 1 - \left[1 + \frac{\theta_1 x}{1 + \theta_1} \right] e^{-\theta_1 x} \right\} + (1 - p) \left\{ 1 - \left[1 + \frac{\theta_2 x}{1 + \theta_2} \right] e^{-\theta_2 x} \right\} \\ &= 1 - p \left[1 + \frac{\theta_1 x}{1 + \theta_1} \right] e^{-\theta_1 x} - (1 - p) \left[1 + \frac{\theta_2 x}{1 + \theta_2} \right] e^{-\theta_2 x}. \end{aligned}$$

We have $F_{L-ML}(x; \theta_1, \theta_2, p) = 0$ for $x \leq 0$. This function is the basis for further properties and applications of the L-ML distribution, and an in-depth study is proposed in this article. At the heart of the discussion, we have made a comparison with the study of [3] from an applied point of view.

The rest of the article is divided into the following sections: Section 2 presents the L-ML distribution. Some of its properties are given in Section 3; Section 4 discusses estimation and simulation; Section 5 proposes several applications to the analysis of three well-referenced real-world data sets. Finally, Section 6 provides some concluding remarks.

2 Definition

Immediately from Equation (3), the probability density function (PDF) of the L-ML distribution is obtained as

$$f_{L-ML}(x; \theta_1, \theta_2, p) = p f_L(x; \theta_1) + (1 - p) f_{ML}(x; \theta_2), \quad x \in \mathbb{R},$$

where $f_L(x; \theta_1)$ and $f_{ML}(x; \theta_2)$ are the PDFs of the L and ML distributions with parameters θ_1 and θ_2 , respectively. That is, for $x > 0$, we have

$$f_{L-ML}(x; \theta_1, \theta_2, p) = p \frac{\theta_1^2}{1 + \theta_1} (1 + x) e^{-\theta_1 x} + (1 - p) \frac{\theta_2}{1 + \theta_2} \left[(1 + \theta_2) e^{\theta_2 x} + 2\theta_2 x - 1 \right] e^{-2\theta_2 x}.$$

This completed by $f_{L-ML}(x; \theta_1, \theta_2, p) = 0$ for $x \leq 0$.

At the boundaries of the support, it can be noticed that

$$f_{L-ML}(0; \theta_1, \theta_2, p) = p \frac{\theta_1^2}{1 + \theta_1} + (1 - p) \frac{\theta_2}{1 + \theta_2} (1 + \theta_2 - 1),$$

showing the interaction of all the parameters at the initial value, and

$$\lim_{x \rightarrow +\infty} f_{L-ML}(x; \theta_1, \theta_2, p) = 0,$$

for all the values of the parameters.

The shape of the PDF $f_{L-ML}(x; \theta_1, \theta_2, p)$ can be studied analytically. However, given its complexity, we have chosen to provide a graphical analysis, mainly to illustrate its functional flexibility. For this PDF, Figure 1 shows plots of unimodal, decreasing and decreasing-increasing-decreasing shapes.

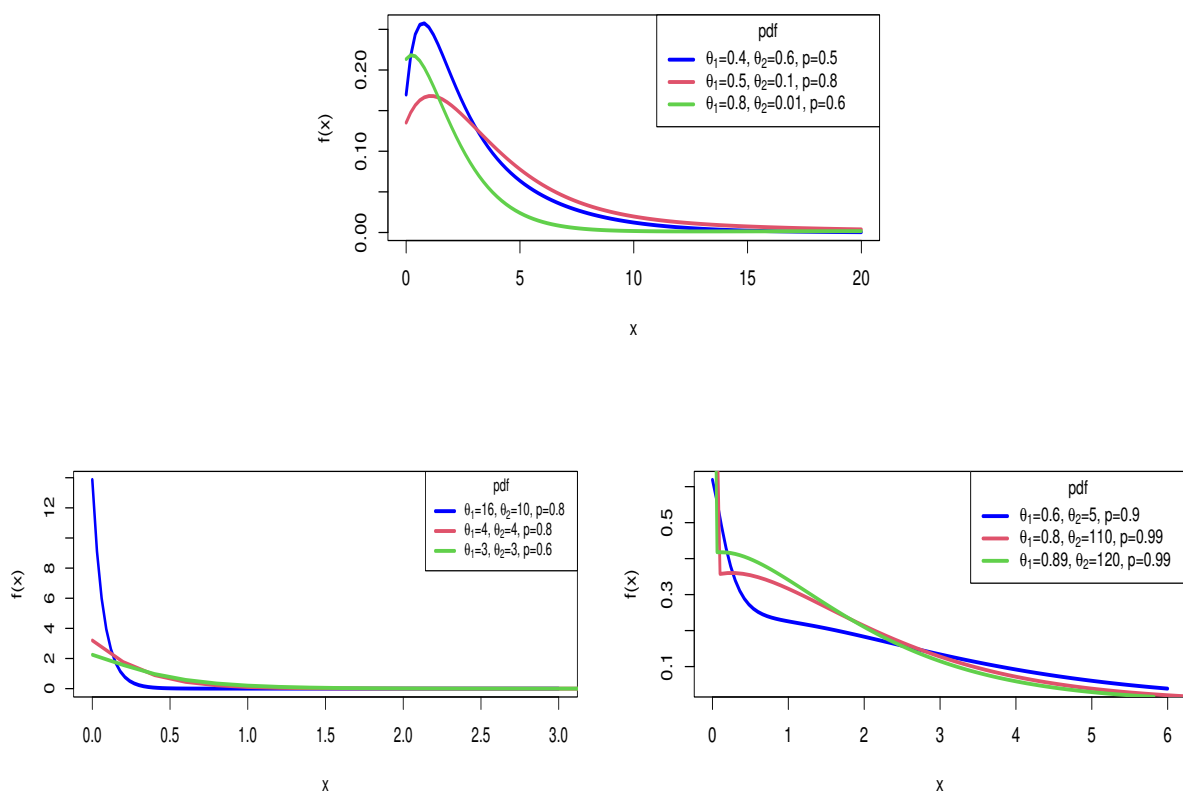


Fig. 1: Graphs of the PDF of the L-ML distribution for different values of parameters

These figures therefore show a wide variety of non-monotonic shapes. Compared to the L-L distribution, we can see that the PDF of the L-ML distribution has decreasing-increasing-decreasing shapes, whereas the PDF of the L-L distribution does not, but has alternative bimodal shapes (see [3, Figure 1]). In addition, the L-ML distribution is clearly more flexible in this respect than the L and ML distributions.

As a complementary reliability function, the HRF of the L-ML distribution needs investigation. To begin, it is expressed as follows:

$$h_{L-ML}(x; \theta_1, \theta_2, p) = \frac{f_{L-ML}(x; \theta_1, \theta_2, p)}{1 - F_{L-ML}(x; \theta_1, \theta_2, p)} = \frac{pf_L(x; \theta_1) + (1 - p)f_{ML}(x; \theta_2)}{1 - [pF_L(x; \theta_1) + (1 - p)F_{ML}(x; \theta_2)]}, \quad x \in \mathbb{R}.$$

Hence, for $x > 0$, it is explicitly defined as

$$h_{L-ML}(x; \theta_1, \theta_2, p) = \frac{p\theta_1^2(1+x)e^{-\theta_1x}/(1+\theta_1) + (1-p)\theta_2 [(1+\theta_2)e^{\theta_2x} + 2\theta_2x - 1] e^{-2\theta_2x}/(1+\theta_2)}{p[1 + \theta_1x/(1+\theta_1)]e^{-\theta_1x} + (1-p)[1 + \theta_2xe^{-\theta_2x}/(1+\theta_2)]e^{-\theta_2x}}.$$

This completed by $h_{L-ML}(x; \theta_1, \theta_2, p) = 0$ for $x \leq 0$.
 As an immediate asymptotic property, we have

$$h_{L-ML}(0; \theta_1, \theta_2, p) = p \frac{\theta_1^2}{1 + \theta_1} + (1 - p) \frac{\theta_2}{1 + \theta_2} (1 + \theta_2 - 1)$$

and

$$\lim_{x \rightarrow +\infty} h_{L-ML}(x; \theta_1, \theta_2, p) = \begin{cases} \theta_1 & \text{if } \theta_2 > \theta_1 \\ \theta_2 & \text{otherwise} \end{cases} .$$

Regarding the PDF, due to its complexity, we have chosen to present a graphical analysis of this HRF, mainly to highlight its functional adaptability. Figure 2 shows different types of unimodal shapes, decreasing and decreasing-increasing-decreasing shapes.

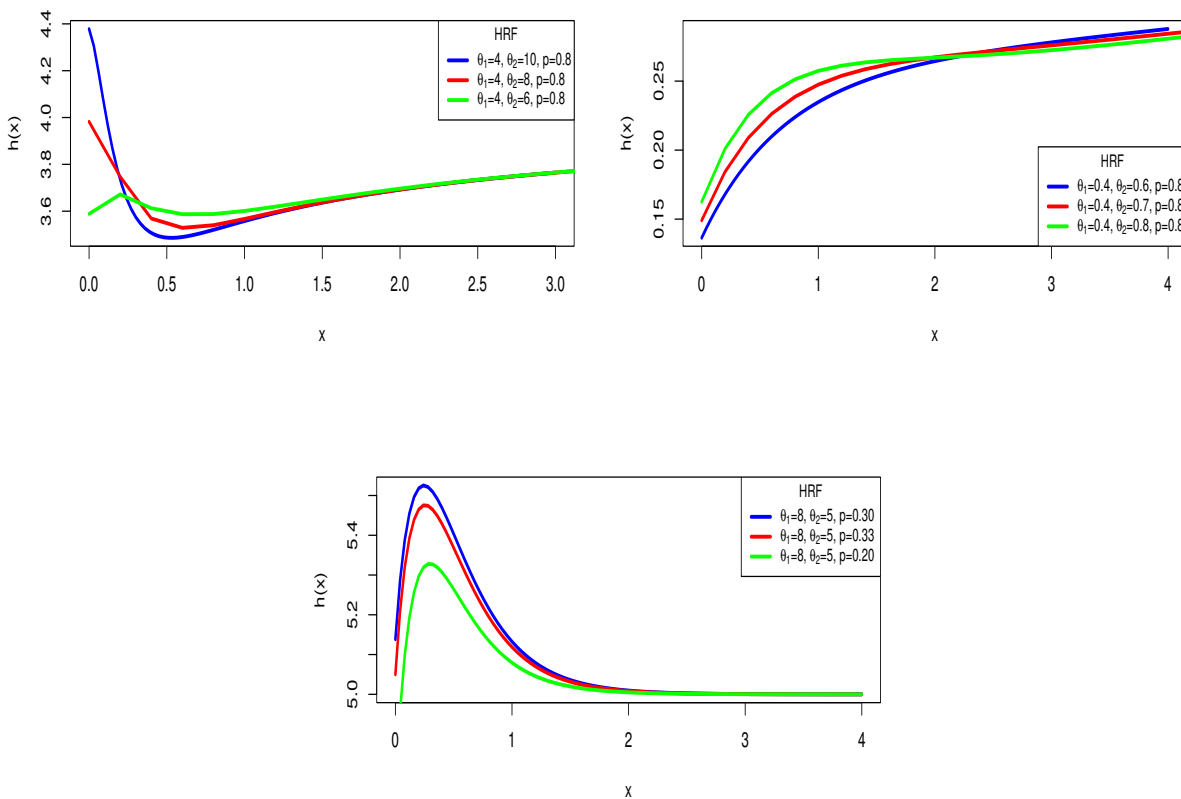


Fig. 2: Graphs of the HRF of the L-ML distribution for different values parameters

There are many monotonic shapes in the figure above. Thus, the HRF of the L-ML distribution is much more adaptive than the HRFs of the L and ML distributions.

3 Properties of the L-ML distribution

Some notable properties of the L-ML distribution are presented in this section. First, the following first-order stochastic ordering property holds: for any $x \in \mathbb{R}$, we have

$$F_{L-ML}(x; \theta_1, \theta_2, p) \geq F_{L-L}(x; \theta_1, \theta_2, p).$$

In this stochastic sense, the CDF functional capabilities of the L-ML distribution "are over" those of the L-L distribution, which may imply different goals in terms of statistical modeling.

Now, let X_1 be a random variable having the L distribution with parameter θ_1 , X_2 be a random variable having the ML distribution with parameter θ_2 , and Y be a random variable having the Bernoulli distribution with parameter $p \in (0, 1)$. These three random variables are supposed to be independent. Then, the following mixture random variable:

$$X = YX_1 + (1 - Y)X_2$$

has the L-ML distribution. As a result, for any measurable function $\psi(x)$ for which the introduced quantity exists, one can observe that

$$\mathbb{E}(\psi(X)) = \mathbb{E}(\mathbb{E}(\psi(X) | Y)) = p\mathbb{E}(\psi(X_1)) + (1 - p)\mathbb{E}(\psi(X_2)),$$

where \mathbb{E} denotes the classical expectation operator and $\mathbb{E}(\cdot | Y)$ denotes the conditional expectation operator with respect to Y . Several properties of the L-ML distribution can be derived from this moment formula. Some of these are described below.

-For any positive integer r , the r -th ordinary moment of X may be expressed in terms of the r -th ordinary moments of X_1 and X_2 as

$$\mathbb{E}(X^r) = p\mathbb{E}(X_1^r) + (1 - p)\mathbb{E}(X_2^r).$$

Hence, based on the existing formulas for the r -th ordinary moment of the L and ML distributions, we have

$$\mathbb{E}(X^r) = r! \left[p \frac{\theta_1 + r + 1}{\theta_1^r(1 + \theta_1)} + (1 - p) \frac{1}{\theta_2^r} \left(1 + \frac{r}{2^{r+1}(1 + \theta_2)} \right) \right].$$

In particular, the mean of X is obtained as

$$\mathbb{E}(X) = p \frac{\theta_1 + 2}{\theta_1(1 + \theta_1)} + (1 - p) \frac{1}{\theta_2} \left(1 + \frac{1}{4(1 + \theta_2)} \right).$$

Using the previous formula and the expression of $\mathbb{E}(X)$, the variance of X is given by

$$\begin{aligned} \mathbb{V}(X) &= 2 \left[p \frac{\theta_1 + 3}{\theta_1^2(1 + \theta_1)} + (1 - p) \frac{1}{\theta_2^2} \left(1 + \frac{2}{8(1 + \theta_2)} \right) \right] \\ &\quad - \left[p \frac{\theta_1 + 2}{\theta_1(1 + \theta_1)} + (1 - p) \frac{1}{\theta_2} \left(1 + \frac{1}{4(1 + \theta_2)} \right) \right]^2. \end{aligned}$$

There is no condensed expression for this variance.

-The r -th central moment of X is given by

$$\begin{aligned} m(r) &= \mathbb{E}((X - \mathbb{E}(X))^r) = \sum_{k=0}^r \binom{r}{k} (-1)^{r-k} \mathbb{E}(X^k) \mathbb{E}(X)^{r-k} \\ &= r! \sum_{k=0}^r \frac{(-1)^{r-k}}{(r-k)!} \left[p \frac{\theta_1 + k + 1}{\theta_1^k(1 + \theta_1)} + (1 - p) \frac{1}{\theta_2^k} \left(1 + \frac{k}{2^{k+1}(1 + \theta_2)} \right) \right] \times \\ &\quad \left[p \frac{\theta_1 + 2}{\theta_1(1 + \theta_1)} + (1 - p) \frac{1}{\theta_2} \left(1 + \frac{1}{4(1 + \theta_2)} \right) \right]^{r-k}. \end{aligned}$$

Thanks to this formula, we can easily calculate the coefficient of skewness, which is given as $SK = m(3)/\mathbb{V}(X)^{3/2}$ and the coefficient of kurtosis, which is given as $KU = m(4)/\mathbb{V}(X)^2$. The expressions for these moment measures are very large, but can be easily calculated numerically using mathematical software (by varying the values of the parameters).

-The moment generating function of X may be expressed in terms of the moment generating functions of X_1 and X_2 as

$$M(t) = \mathbb{E}(e^{tX}) = p\mathbb{E}(e^{tX_1}) + (1 - p)\mathbb{E}(e^{tX_2}), \quad t \in (-\infty, \min(\theta_1, \theta_2, p)).$$

Hence, based on the existing formulas for the moment generating functions of the L and ML distributions, we have

$$M(t) = p \frac{\theta_1^2(\theta_1 - t + 1)}{(1 + \theta_1)(\theta_1 - t)^2} + (1 - p) \left[\frac{\theta_2}{\theta_2 - t} + \frac{t\theta_2}{(1 + \theta_2)(2\theta_2 - t)^2} \right], \quad t \in (-\infty, \min(\theta_1, \theta_2, p)).$$

–The characteristic function of X may be expressed in terms of the characteristic functions of X_1 and X_2 as

$$\varphi(t) = \mathbb{E}(e^{itX}) = p\mathbb{E}(e^{itX_1}) + (1-p)\mathbb{E}(e^{itX_2}), \quad t \in \mathbb{R},$$

where i is the imaginary unit, i.e., such that $i^2 = -1$. Rudely written, we have $\varphi(t) = M(it)$, which gives

$$\varphi(t) = p \frac{\theta_1^2(\theta_1 - it + 1)}{(1 + \theta_1)(\theta_1 - it)^2} + (1-p) \left[\frac{\theta_2}{\theta_2 - it} + \frac{it\theta_2}{(1 + \theta_2)(2\theta_2 - it)^2} \right], \quad t \in \mathbb{R}.$$

Many mathematical or statistical manipulations of the L-ML distribution can be made using all these probabilistic measures.

4 Estimation and simulation

In this section, we derive the unknown parameters of the L-ML distribution using the maximum likelihood method. Based on n Observations of a random variable X having the L-LM distribution, say $X_1 || dots, x_n$, this method consists of estimating the parameters θ_1 , θ_2 and p by $\hat{\theta}_1$, $\hat{\theta}_2$ and \hat{p} , such that

$$(\hat{\theta}_1, \hat{\theta}_2, \hat{p}) = \operatorname{argmax}_{(\theta_1, \theta_2, p) \in [0, +\infty]^2 \times [0, 1]} \log L(\theta_1, \theta_2, p),$$

where $L(\theta_1, \theta_2, p)$ denotes the likelihood function defined by

$$L(\theta_1, \theta_2, p) = \prod_{i=1}^n f_{L-ML}(x_i; \theta_1, \theta_2, p),$$

so that

$$\log L(\theta_1, \theta_2, p) = \sum_{i=1}^n \log \left[p \frac{\theta_1^2}{1 + \theta_1} (1 + x_i) e^{-\theta_1 x_i} + (1-p) \frac{\theta_2}{1 + \theta_2} \left[(1 + \theta_2) e^{\theta_2 x_i} + 2\theta_2 x_i - 1 \right] e^{-2\theta_2 x_i} \right].$$

The estimates obtained are called the maximum likelihood estimates (MLEs). Once they are obtained, adopting the substitution approach, the estimated PDF of the L-ML distribution is given as $f_{L-ML}(x; \hat{\theta}_1, \hat{\theta}_2, \hat{p})$, and the estimated CDF of the L-ML distribution is given as $F_{L-ML}(x; \hat{\theta}_1, \hat{\theta}_2, \hat{p})$. Similarly, the estimated HRF of the L-ML distribution is given as $h_{L-ML}(x; \hat{\theta}_1, \hat{\theta}_2, \hat{p})$.

We now examine the performance of the MLEs using a Monte Carlo simulation study for selected values of the parameters θ_1 , θ_2 , and p . The simulation experiment was repeated 100,000 times each with sample sizes of $n = 10, 20, \dots, 100$, and the parameter combinations are chosen as follows:

- SET 1: $\theta_1 = 1$, $\theta_2 = 1$, and $p = 0.5$
- SET 2: $\theta_1 = 2$, $\theta_2 = 2$, and $p = 0.5$
- SET 3: $\theta_1 = 1.5$, $\theta_2 = 1.5$, and $p = 0.5$

We therefore study the numerical properties of the corresponding MLEs, biases, mean square errors (MSEs), lower bound (LB), upper bound (UB), and coverage probability (CP) with respect to the 95% confidence interval of the parameters. Tables 1, ?? and 3 show the simulation results for SET 1, SET 2 and SET 3 respectively. The R software [23] was used for the calculations.

From these tables, we can see that the biases and MSEs decrease as the sample size increases. Therefore, the estimation approach considered works effectively for estimating the parameters of the L-ML model. Figure 3 graphically shows the shapes of the biases for the MLEs for n , which varies continuously from 10 to 100, by taking certain values of the parameters.

Table 1: Simulation results for SET 1

| n | Parameter | MLE | Bias | MSE | CP | LB | UB |
|-----|------------|-------|--------|-------|-------|-------|-------|
| 10 | θ_1 | 1.114 | 0.114 | 0.187 | 0.923 | 0.856 | 1.372 |
| | θ_2 | 1.399 | 0.399 | 2.167 | 0.977 | 0.521 | 2.278 |
| | p | 0.391 | -0.109 | 0.179 | 0.962 | 0.138 | 0.645 |
| 20 | θ_1 | 1.056 | 0.056 | 0.165 | 0.925 | 0.880 | 1.232 |
| | θ_2 | 1.332 | 0.332 | 1.650 | 0.932 | 0.760 | 1.904 |
| | p | 0.411 | -0.089 | 0.170 | 0.944 | 0.234 | 0.587 |
| 30 | θ_1 | 1.044 | 0.044 | 0.159 | 0.932 | 0.902 | 1.185 |
| | θ_2 | 1.315 | 0.315 | 1.567 | 0.909 | 0.856 | 1.773 |
| | p | 0.424 | -0.076 | 0.165 | 0.927 | 0.281 | 0.567 |
| 40 | θ_1 | 1.027 | 0.027 | 0.150 | 0.940 | 0.896 | 1.159 |
| | θ_2 | 1.311 | 0.311 | 1.500 | 0.885 | 0.982 | 1.695 |
| | p | 0.434 | -0.066 | 0.160 | 0.921 | 0.312 | 0.556 |
| 50 | θ_1 | 1.024 | 0.024 | 0.140 | 0.945 | 0.916 | 1.133 |
| | θ_2 | 1.306 | 0.306 | 1.500 | 0.895 | 0.949 | 1.663 |
| | p | 0.439 | -0.061 | 0.154 | 0.915 | 0.331 | 0.546 |
| 60 | θ_1 | 1.024 | 0.024 | 0.130 | 0.943 | 0.928 | 1.119 |
| | θ_2 | 1.300 | 0.300 | 1.460 | 0.889 | 0.982 | 1.617 |
| | p | 0.446 | -0.054 | 0.154 | 0.915 | 0.348 | 0.545 |
| 70 | θ_1 | 1.021 | 0.021 | 0.120 | 0.944 | 0.936 | 1.107 |
| | θ_2 | 1.290 | 0.290 | 1.450 | 0.882 | 0.999 | 1.622 |
| | p | 0.446 | -0.054 | 0.150 | 0.901 | 0.356 | 0.536 |
| 80 | θ_1 | 1.017 | 0.017 | 0.125 | 0.953 | 0.933 | 1.101 |
| | θ_2 | 1.276 | 0.276 | 1.400 | 0.880 | 1.001 | 1.539 |
| | p | 0.445 | -0.055 | 0.148 | 0.916 | 0.362 | 0.528 |
| 90 | θ_1 | 1.016 | 0.016 | 0.120 | 0.952 | 0.936 | 1.110 |
| | θ_2 | 1.270 | 0.270 | 1.375 | 0.878 | 1.023 | 1.529 |
| | p | 0.448 | -0.052 | 0.144 | 0.909 | 0.370 | 0.525 |
| 100 | θ_1 | 1.014 | 0.014 | 0.110 | 0.952 | 0.951 | 1.081 |
| | θ_2 | 1.250 | 0.250 | 1.350 | 0.875 | 1.019 | 1.481 |
| | p | 0.455 | -0.045 | 0.141 | 0.908 | 0.382 | 0.528 |

Table 2: Simulation results for SET 2

| n | Parameter | MLE | Bias | CP | LB | UB |
|-----|------------|-------|--------|-------|-------|-------|
| 10 | θ_1 | 2.184 | 0.184 | 0.950 | 1.750 | 2.620 |
| | θ_2 | 2.488 | 0.488 | 0.930 | 2.100 | 2.880 |
| | p | 0.376 | -0.124 | 0.940 | 0.320 | 0.430 |
| 20 | θ_1 | 2.103 | 0.103 | 0.960 | 1.880 | 2.330 |
| | θ_2 | 2.446 | 0.446 | 0.940 | 2.190 | 2.700 |
| | p | 0.401 | -0.099 | 0.950 | 0.360 | 0.440 |
| 30 | θ_1 | 2.090 | 0.090 | 0.970 | 1.920 | 2.260 |
| | θ_2 | 2.418 | 0.418 | 0.950 | 2.210 | 2.630 |
| | p | 0.405 | -0.095 | 0.960 | 0.370 | 0.440 |
| 40 | θ_1 | 1.920 | -0.080 | 0.980 | 1.760 | 2.080 |
| | θ_2 | 2.398 | 0.398 | 0.960 | 2.200 | 2.600 |
| | p | 0.419 | -0.081 | 0.970 | 0.380 | 0.450 |
| 50 | θ_1 | 1.975 | -0.025 | 0.980 | 1.850 | 2.100 |
| | θ_2 | 2.354 | 0.354 | 0.970 | 2.180 | 2.520 |
| | p | 0.424 | -0.076 | 0.970 | 0.390 | 0.450 |
| 60 | θ_1 | 1.977 | -0.023 | 0.990 | 1.860 | 2.100 |
| | θ_2 | 2.359 | 0.359 | 0.970 | 2.190 | 2.530 |
| | p | 0.427 | -0.073 | 0.980 | 0.390 | 0.450 |

| n | Parameter | MLE | Bias | CP | LB | UB |
|-----|------------|-------|--------|-------|-------|-------|
| 70 | θ_1 | 1.975 | -0.025 | 0.990 | 1.870 | 2.090 |
| | θ_2 | 2.324 | 0.324 | 0.980 | 2.160 | 2.490 |
| | p | 0.428 | -0.072 | 0.980 | 0.390 | 0.460 |
| 80 | θ_1 | 1.976 | -0.024 | 0.990 | 1.870 | 2.090 |
| | θ_2 | 2.317 | 0.317 | 0.980 | 2.150 | 2.480 |
| | p | 0.429 | -0.071 | 0.980 | 0.390 | 0.460 |
| 90 | θ_1 | 1.977 | -0.023 | 0.990 | 1.880 | 2.090 |
| | θ_2 | 2.292 | 0.292 | 0.980 | 2.130 | 2.450 |
| | p | 0.435 | -0.065 | 0.980 | 0.400 | 0.460 |
| 100 | θ_1 | 1.960 | -0.040 | 0.990 | 1.850 | 2.070 |
| | θ_2 | 2.200 | 0.200 | 0.980 | 2.050 | 2.350 |
| | p | 0.440 | -0.060 | 0.980 | 0.410 | 0.470 |

Table 3: Simulation results for SET 3

| n | Parameter | MLE | Bias | MSE | CP | LB | UB |
|-----|------------|-------|--------|-------|-------|-------|-------|
| 10 | θ_1 | 1.748 | 0.248 | 0.745 | 0.914 | 1.236 | 2.260 |
| | θ_2 | 1.920 | 0.420 | 2.203 | 0.977 | 1.038 | 2.803 |
| | p | 0.373 | -0.127 | 0.186 | 0.948 | 0.118 | 0.628 |
| 20 | θ_1 | 1.559 | 0.059 | 0.229 | 0.924 | 1.351 | 1.767 |
| | θ_2 | 1.899 | 0.399 | 2.143 | 0.931 | 1.282 | 2.517 |
| | p | 0.401 | -0.099 | 0.176 | 0.950 | 0.222 | 0.579 |
| 30 | θ_1 | 1.529 | 0.029 | 0.192 | 0.928 | 1.373 | 1.685 |
| | θ_2 | 1.906 | 0.406 | 2.197 | 0.906 | 1.396 | 2.416 |
| | p | 0.421 | -0.079 | 0.169 | 0.939 | 0.276 | 0.565 |
| 40 | θ_1 | 1.518 | 0.018 | 0.189 | 0.934 | 1.383 | 1.652 |
| | θ_2 | 1.879 | 0.379 | 2.096 | 0.891 | 1.446 | 2.312 |
| | p | 0.425 | -0.075 | 0.165 | 0.940 | 0.301 | 0.548 |
| 50 | θ_1 | 1.518 | 0.018 | 0.180 | 0.942 | 1.400 | 1.636 |
| | θ_2 | 1.841 | 0.341 | 1.911 | 0.890 | 1.469 | 2.212 |
| | p | 0.430 | -0.070 | 0.163 | 0.937 | 0.320 | 0.540 |
| 60 | θ_1 | 1.504 | 0.014 | 0.176 | 0.940 | 1.398 | 1.610 |
| | θ_2 | 1.841 | 0.341 | 1.873 | 0.877 | 1.506 | 2.177 |
| | p | 0.432 | -0.068 | 0.160 | 0.934 | 0.332 | 0.531 |
| 70 | θ_1 | 1.512 | 0.012 | 0.191 | 0.947 | 1.409 | 1.614 |
| | θ_2 | 1.824 | 0.324 | 1.808 | 0.875 | 1.519 | 2.130 |
| | p | 0.437 | -0.063 | 0.158 | 0.933 | 0.345 | 0.529 |
| 80 | θ_1 | 1.506 | 0.006 | 0.174 | 0.944 | 1.415 | 1.597 |
| | θ_2 | 1.792 | 0.317 | 1.645 | 0.874 | 1.518 | 2.066 |
| | p | 0.434 | -0.055 | 0.157 | 0.938 | 0.348 | 0.519 |
| 90 | θ_1 | 1.497 | -0.003 | 0.200 | 0.945 | 1.405 | 1.590 |
| | θ_2 | 1.799 | 0.299 | 1.695 | 0.865 | 1.538 | 2.061 |
| | p | 0.435 | -0.051 | 0.152 | 0.939 | 0.356 | 0.514 |
| 100 | θ_1 | 1.503 | 0.003 | 0.200 | 0.949 | 1.413 | 1.592 |
| | θ_2 | 1.809 | 0.190 | 1.625 | 0.870 | 1.559 | 2.059 |
| | p | 0.446 | -0.049 | 0.151 | 0.936 | 0.370 | 0.521 |

The observations noted are for the particular initial values of θ_1 , θ_2 and p , but the same observations held for a wide range of other values of θ_1 , θ_2 and p . In particular, the magnitude of the biases always decreased to zero as n increased, and the MSE always decreased to zero as n increased. Therefore, the MLEs $\hat{\theta}_1$, $\hat{\theta}_2$ and \hat{p} associated with the L-ML distribution can be considered to behave according to the large sample theory of the MLE.

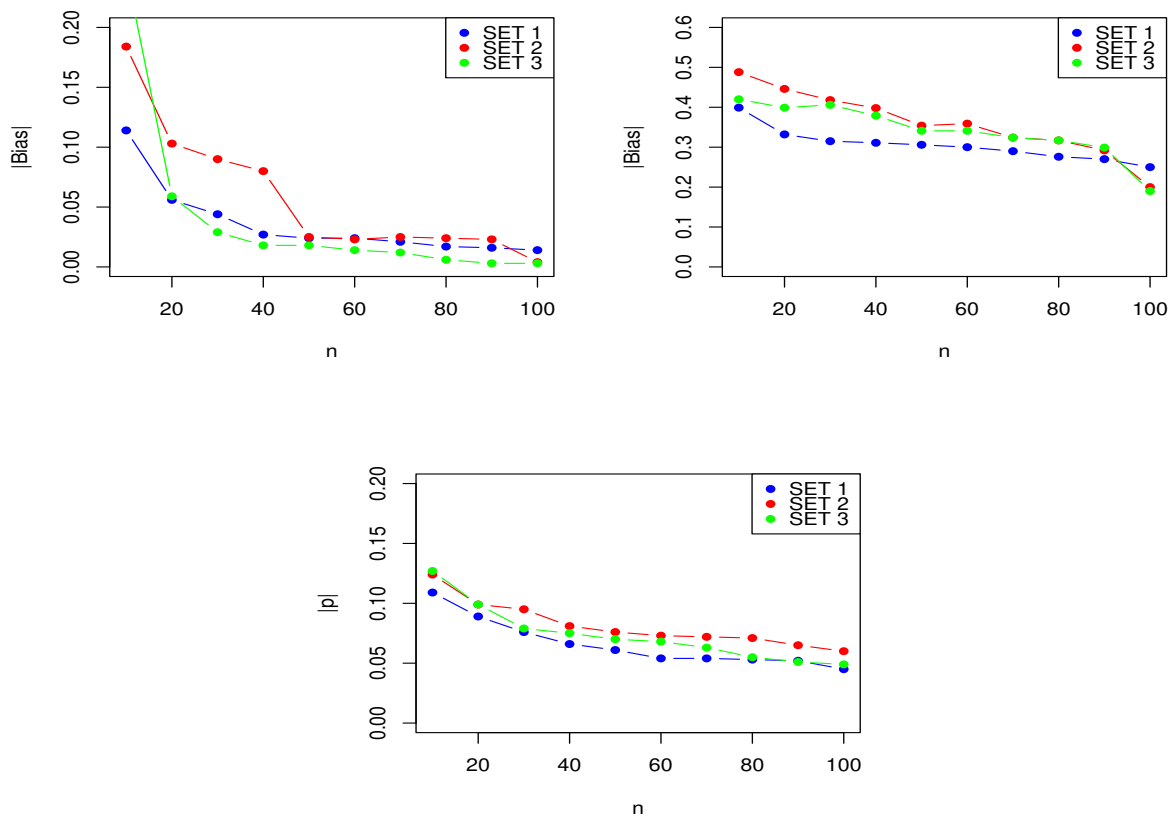


Fig. 3: Plots illustrating the biases of the estimated parameters θ_1 , θ_2 and p , respectively. The first graph depicts the biases associated with θ_1 , the second associated with θ_2 , and the third associated with p .

5 Applications

5.1 Framework

In this section, we use three real data sets to demonstrate the capabilities of the proposed model. To do this, we compare the adaptability of the L-ML model with that of the L-L model by [3].

To check the goodness-of-fit, we derive the unknown parameters using the maximum likelihood method, maximized $-\log$ -likelihood ($-\log L_{ik}$), and compare the values of the Akaike information criterion (AIC) and Bayesian information criterion (BIC), the values of the Kolmogorov-Smirnov (K-S) statistic, the corresponding p -values, and the values of the Anderson-Darling (A^*) and Cramér-von Mises (W^*). They are evaluated using the R software via the commands FITDIST(), KS.TEST(), AD.TEST() and CVM.TEST().

5.2 Data Set 1 (Bladder cancer data)

The real data set presents the remission times (in months) of a random sample of 128 bladder cancer patients, which has been given by [12]. Several authors have studied this data set. See [16] for further information. The data are displayed as follows:

0.08, 2.09, 3.48, 4.87, 6.94, 8.66, 13.11, 23.63, 0.20, 2.23, 3.52, 4.98, 6.97, 9.02, 13.29, 0.40, 2.26, 3.57, 5.06, 7.09, 9.22, 13.80, 25.74, 0.50, 2.46, 3.64, 5.09, 7.26, 9.47, 14.24, 25.82, 0.51, 2.54, 3.70, 5.17, 7.28, 9.74, 14.76, 26.31, 0.81, 2.62, 3.82, 5.32, 7.32, 10.06, 14.77, 32.15, 2.64, 3.88, 5.32, 7.39, 10.34, 14.83, 34.26, 0.90, 2.69, 4.18, 5.34, 7.59, 10.66, 15.96, 36.66, 1.05, 2.69, 4.23, 5.41, 7.62, 10.75, 16.62, 43.01, 1.19, 2.75, 4.26, 5.41, 7.63, 17.12, 46.12, 1.26, 2.83, 4.33, 5.49,

7.66, 11.25, 17.14, 79.05, 1.35, 2.87, 5.62, 7.87, 11.64, 17.36, 1.40, 3.02, 4.34, 5.71, 7.93, 11.79, 18.10, 1.46, 4.40, 5.85, 8.26, 11.98, 19.13, 1.76, 3.25, 4.50, 6.25, 8.37, 12.02, 2.02, 3.31, 4.51, 6.54, 8.53, 12.03, 20.28, 2.02, 3.36, 6.76, 12.07, 21.73, 2.07, 3.36, 6.93, 8.65, 12.63, 22.69.

The results of the descriptive investigation for the fitted L-ML and L-L models for data set 1 are summarized in Table 4.

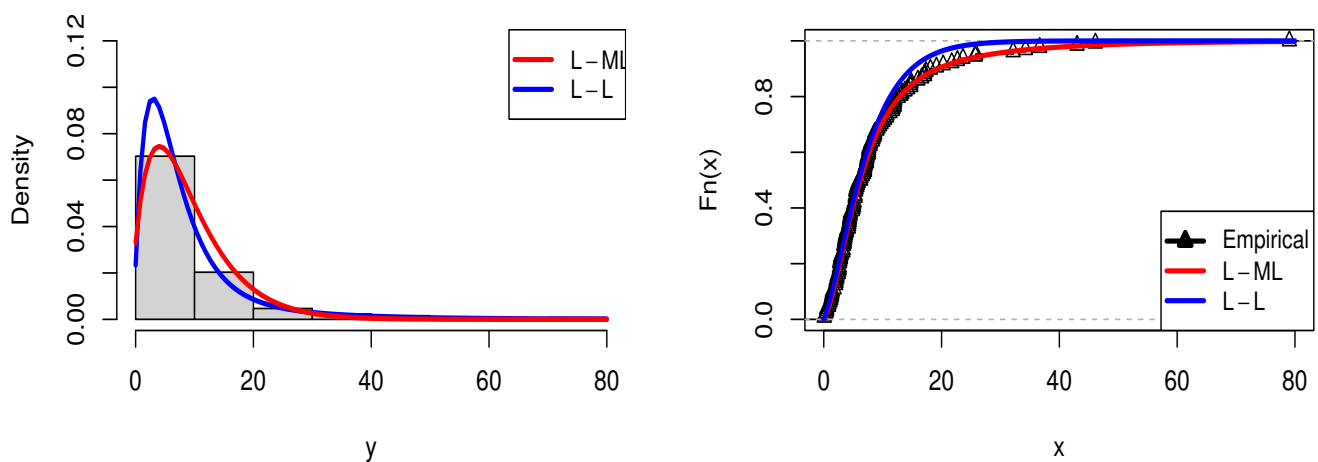
Table 4: Estimated values, $-\log L_{ik}$, AIC, BIC, K-S statistics, p -value, A^* and W^* for data set 1

| Model | Estimates | $-\log L_{ik}$ | AIC | BIC | K-S | p -value | A^* | W^* |
|-------|--|----------------|----------|----------|----------|------------|----------|---------|
| L-ML | $\hat{\theta}_1 = 0.0529$ $\hat{\theta}_2 = 0.1780$ $\hat{p} = 0.1443$ | 406.7274 | 819.4547 | 828.0108 | 0.027029 | 0.9999 | 0.093177 | 0.0116 |
| L-L | $\hat{\theta}_1 = 0.1991$ $\hat{\theta}_2 = 0.2569$ $\hat{p} = 0.1469$ | 416.8962 | 839.7925 | 848.3486 | 0.071674 | 0.5265 | 2.9633 | 0.38142 |

From the study, the smallest $-\log L_{ik}$, AIC, BIC, K-S statistic, A^* , W^* and the highest p -values are found for the L-ML model, so far. It can therefore be considered as the best.

The estimated PDFs and CDFs of the L-L and L-ML models are plotted in Figure 4.

Fig. 4: Plots of the estimated PDFs and the estimated CDFs of the L-L and L-ML models for data set 1



From this figure, we see that the fitted PDF for the L-ML model is closer to the empirical histogram than the fits for the L-L model.

5.3 Data Set 2 (Vinyl chloride data)

Data set 2 presents the vinyl chloride data obtained from clean upgradient monitoring wells in mg/l, provided by [4]. The data are:

5.1, 1.2, 1.3, 0.6, 0.5, 2.4, 0.5, 1.1, 8, 0.8, 0.4, 0.6, 0.9, 0.4, 2, 0.5, 5.3, 3.2, 2.7, 2.9, 2.5, 2.3, 1, 0.2, 0.1, 0.1, 1.8, 0.9, 2, 4, 6.8, 1.2, 0.4, 0.2.

The studied statistical parameters are listed in Table 5.

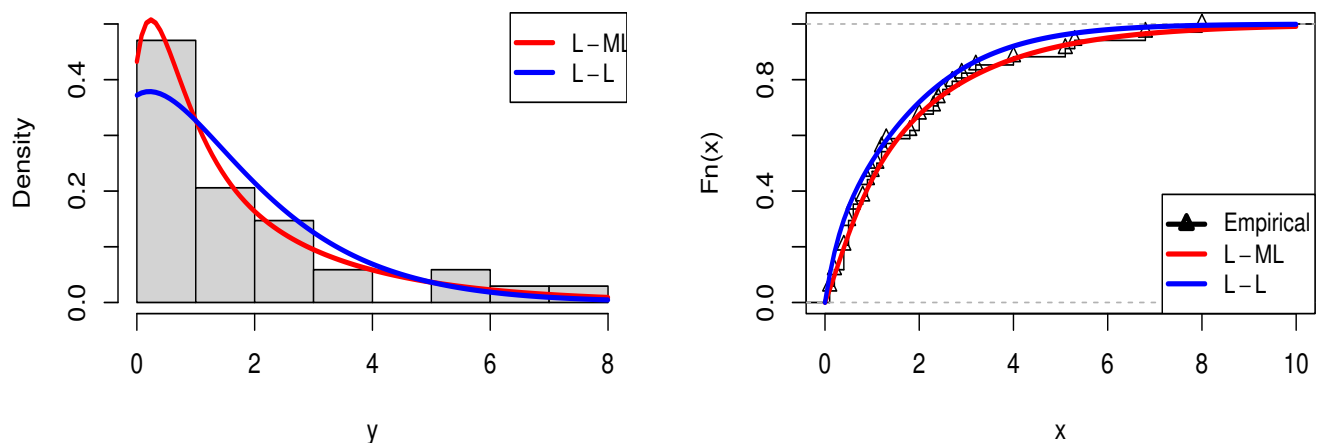
Table 5: Estimated values, $-\log L_{ik}$, AIC, BIC, K-S statistics, p -value, A^* and W^* for data set 2

| Models | Estimates | $-\log L_{ik}$ | AIC | BIC | K-S | p -value | A^* | W^* |
|--------|---|----------------|----------|----------|----------|------------|---------|----------|
| L-ML | $\hat{\theta}_1 = 0.4199$ $\hat{\theta}_2 = 1.3799$ $\hat{\rho} = 0.5437$ | 55.05361 | 116.1072 | 120.6863 | 0.078915 | 0.9839 | 0.18398 | 0.024671 |
| L-L | $\hat{\theta}_1 = 0.8238$ $\hat{\theta}_2 = 4.3997$ $\hat{\rho} = 0.7650$ | 56.30364 | 118.6073 | 123.1864 | 0.17907 | 0.2256 | 1.4339 | 0.23251 |

From Table 5, the smallest $-\log L_{ik}$, AIC, BIC, K-S statistic, A^* , W^* and the highest p -values are found for the L-ML model. It can therefore be considered as the best.

The estimated PDFs and CDFs of the L-L and L-ML models are shown in Figure 5.

Fig. 5: Plots of the estimated PDFs and the estimated CDFs of the L-L and L-ML models for data set 2



From this figure, we see that the fitted PDF for the L-ML model is closer to the empirical histogram than the fits for the L-L model. In addition, the empirical CDF is very close to the fitted CDF. Looking at these plots, it is clear that the L-ML model outperforms the L-L model in terms of model fit.

5.4 Data Set 3 (Wheaton river flood data)

Data set 3 consists of 72 exceedances of flood peaks (in m3 /s) of the Wheaton river near Carcross in Yukon Territory, Canada for the years 1958-1984, provided by [7]. The data are:
 1.7, 2.2, 14.4, 1.1, 0.4, 20.6, 5.3, 0.7, 1.9, 13.0, 12.0, 9.3, 1.4, 18.7, 8.5, 25.5, 11.6, 14.1, 22.1, 1.1, 2.5, 27.0, 14.4, 1.7, 37.6, 0.6, 2.2, 39.0, 0.3, 15.0, 11.0, 7.3, 22.9, 1.7, 0.1, 1.1, 0.6, 9.0, 1.7, 7.0, 20.1, 0.4, 2.8, 14.1, 9.9, 10.4, 10.7, 30.0.

Table 6 displays the considered statistical measures.

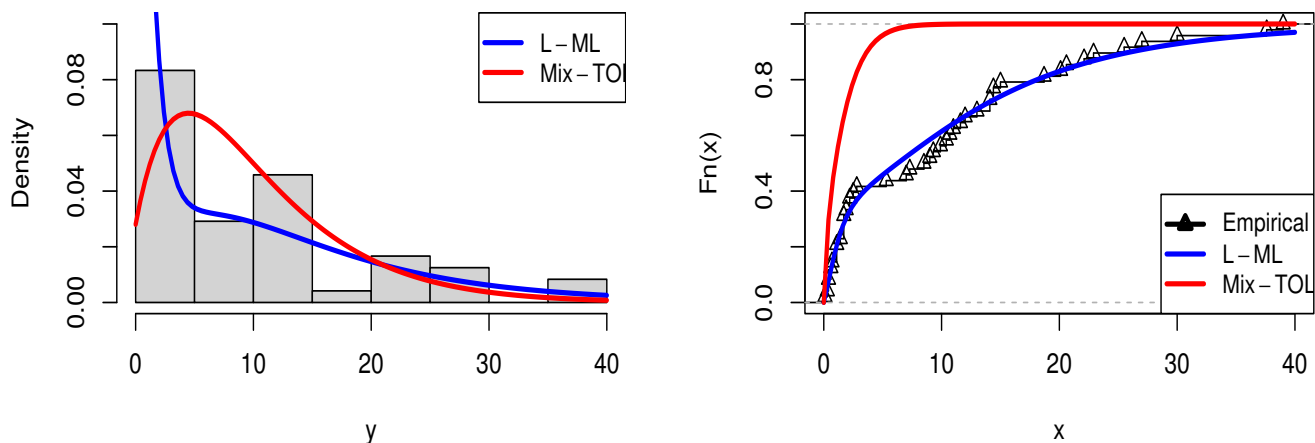
Table 6: Estimated values, $-\log L_{ik}$, AIC, BIC, K-S statistics, p -value, A^* and W^* for data set 3

| Models | Estimates | $-\log L_{ik}$ | AIC | BIC | K-S | p -value | A^* | W^* |
|--------|---|----------------|----------|----------|----------|------------|---------|----------|
| L-ML | $\hat{\theta}_1 = 0.0795$ $\hat{\theta}_2 = 0.8798$ $\hat{\rho} = 0.6409$ | 153.905 | 313.8101 | 319.4237 | 0.078915 | 0.9839 | 0.18398 | 0.024671 |
| L-L | $\hat{\theta}_1 = 0.8096$ $\hat{\theta}_2 = 0.1821$ $\hat{\rho} = 0.6125$ | 167.7116 | 341.4232 | 347.0368 | 0.19202 | 0.05804 | 21.844 | 2.5884 |

From Table 6, the smallest $-\log L_{ik}$, AIC, BIC, K-S statistic, A^* , W^* and the highest p -values are found for the L-ML model. It can therefore be considered as the best.

Figure 6 shows the estimated PDFs and CDFs of the L-L and L-ML models.

Fig. 6: Plots of the estimated PDFs and the estimated CDFs of the L-L and L-ML models for data set 3



From this figure, we see that the fitted PDF for the L-ML model is closer to the empirical histogram than the fits for the L-L model. Examining these plots, it is clear that the L-ML model outperforms the L-L model in terms of model fit. This confirms the performance of the L-ML model.

6 Concluding remarks

In this article, we propose a new mixture distribution, called the L-ML distribution, which is a mixture of the Lindley and modified Lindley distributions in the analysis of data with positive real support. An obvious reason for generalizing a standard distribution is that the generalized form allows greater flexibility in modelling real data. The expansions for the moments and the moment generating function are given. A simulation study is carried out to investigate the maximum likelihood estimation approach. The good results support the use of the L-ML distribution to describe data sets. Three practical applications of the L-ML model show that it can be expected to provide better fits than its main competitor, the L-L distribution.

Declarations

Ethical Responsibilities of Authors: All authors have read, understood, and complied as applicable with the statement on "Ethical responsibilities of Authors" as found in the Instructions for Authors.

Availability of data and material: Not applicable.

Funding: The authors declare that no funds, grants, or other support were received during the preparation of this article.

Consent to Participate: The authors have given consent to participate in and publish this research work.

Consent for publication: The authors have given consent for the publication of this article.

Competing interests: The authors have no relevant financial or non-financial interests to disclose.

Ethics approval and consent to participate: The authors are declaring that the article was not submitted or published anywhere. All the authors have given consent to participate in the publication of this article.

References

- [1] Afify, A.Z., Nassar, M., Cordeiro, G.M. and Kumar, D. (2020). The Weibull Marshall-Olkin Lindley distribution: properties and estimation, *Journal of Taibah University for Science*, 14 (1), 192-204.
- [2] Algarni, A. (2021). On a new generalized Lindley distribution: Properties, estimation and applications. *PLOS ONE*, 16(2): e0244328. <https://doi.org/10.1371/journal.pone.0244328>
- [3] Al-Moisheer, A. S., Daghestani, A. F. and Sultan, K. S. (2020). Mixture of two one-parameter Lindley distributions: properties and estimation. *Journal of Statistical Theory and Practice*, 15(1). doi:10.1007/s42519-020-00133-4
- [4] Bhaumik, D. K., Kapur, K. and Gibbons, R.D. (2009). Testing parameters of a Gamma distribution for small samples. *Technometrics*, 51(3): 326-334.
- [5] Chesneau, C., Tomy, L. and Gillariose, J. (2020). The inverted modified Lindley distribution, *Journal of Statistical Theory and Practice*, 14: 1-17.
- [6] Chesneau, C., Tomy, L. and Gillariose, J. (2021). A new modified Lindley distribution with properties and applications, *Journal of Statistics and Management Systems*, 24(7): 1383-1403.
- [7] Choulakian, V. and Stephens, M. A. (2001). Goodness-of-fit for the generalized Pareto distribution. *Technometrics*, 43(4):478-484.
- [8] Ghitany, M. E., Al-Mutairi, D. K., Balakrishnan, N. and Al-Enezi, L. J. (2013). Power Lindley distribution and associated inference, *Computational Statistics and Data Analysis*, 6: 20-33.
- [9] Guerra, R.R.; Peña-Ramírez, F.A.; Mafalda, C.P.; Cordeiro, G.M. Two-component unit weibull mixture model to analyze vote proportions. *Comput. Sci. Math. Forum* 2023, 7, 45. <https://doi.org/10.3390/IOCMA2023-14550>
- [10] Hassan, A. S., Elgarhy, M., Mohamd, R. E. and Alrajhi, S. (2019). On the alpha power transformed power Lindley distribution, *Journal of Probability and Statistics*, 2019, <https://doi.org/10.1155/2019/8024769>.
- [11] Jewell, N. (1982) Mixtures of exponential distributions. *The Annals of Statistics*, 10(2): 479-484
- [12] Lee, E. T. and Wang, J. W. (2003). *Statistical Methods for Survival Data Analysis*, New York, Wiley.
- [13] Lindley, D. V. (1958). Fiducial distributions and Bayes' theorem, *Journal of the Royal Statistical Society, Series A*, 20, 102-107.
- [14] Murat Bulut, Y., Zehra, F., Gru, D. and Arslan, O. (2021). Alpha Power Lomax Distribution: Properties and Application. *Journal of Reliability and Statistical Studies*, 64, 366-373.
- [15] Nadarajah, S., Bakouch, H. S. and Tahmasbi, R. (2011). A generalized Lindley distribution, *Sankhya B - Applied and Interdisciplinary Statistics*, 73: 331-359.
- [16] Merovci, F. (2013). Transmuted Lindley distribution, *International Journal of Open Problems in Computer Science and Mathematics*, 6: 63-72.
- [17] MirMostafae, S. M. T. K., Alizadeh, M., Altun, E. and Nadarajah, S. (2019). The exponentiated generalized power Lindley distribution: properties and applications, *Applied Mathematics-A Journal of Chinese Universities*, 34(2), 127-148.
- [18] Razali, A. M. and Salih, A. A. (2009) Combining two Weibull distributions using a mixing parameter. *European Journal of Scientific Research*, 31(2):296-305.
- [19] Singh, S. K., Singh, U. and Sharma, V. K. (2014). The truncated Lindley distribution-Inference and application. *Journal of Statistics Applications and Probability*, 3: 219-228.

- [20] Shanker, R. and Mishra, A. (2013). A quasi Lindley distribution. *African Journal of Mathematics and Computer Science Research*, 6: 64-71.
- [21] Shanker, R. and Mishra, A. (2013). A two parameter Lindley distribution. *Statistics in transition new series*, 14: 45-56.
- [22] Sharma, V., Singh, S., Singh, U. and Agiwal, V. (2015). The inverse Lindley distribution: a stress-strength reliability model with applications to head and neck cancer data. *Journal of Industrial and Production Engineering*, 32: 162-173.
- [23] Team, R.C. R: A Language and Environment for Statistical Computing; R Foundation for Statistical Computing: Vienna, Austria, 2020.
- [24] Tomy, L. (2018). A retrospective study on Lindley distribution. *Biometrics and Biostatistics International Journal*, 7: 163-169.
- [25] Tomy, L. and Gillariose, J. (2021). A review on mathematically transformed Lindley random variables, *Biometrics and Biostatistics International Journal*, 10(2): 46-48.
- [26] Wiper, M., Insua, D. and Ruggeri, F. (2001). Mixtures of Gamma distributions with applications. *Journal of Computational and Graphical Statistics*, 10(3):440-454
- [27] Zakerzadeh, H. and Dolati, A. (2009). Generalized Lindley distribution. *Journal of mathematical extension*, 3: 13-25.
- [28] Zeghdoudi, H. and Nedjar, S. (2016). Gamma-Lindley distribution and its application, *Journal of Applied Probability and Statistics*, 11(1), 129-138.
-